

Strong electron-phonon coupling in superconducting MgB₂: A specific heat studyCh. Wälti,¹ E. Felder,¹ C. Degen,¹ G. Wigger,¹ R. Monnier,¹ B. Delley,² and H. R. Ott¹¹Laboratorium für Festkörperphysik, ETH-Hönggerberg, 8093 Zürich, Switzerland²PSI, 5232 Villigen, Switzerland

(Received 5 March 2001; published 16 October 2001)

We report on measurements of the specific heat of the recently discovered superconductor MgB₂ in the temperature range between 3 and 220 K. Based on a modified Debye-Einstein model, we have achieved a rather accurate account of the lattice contribution to the specific heat, which allows us to separate the electronic contribution from the total measured specific heat. From our result for the electronic specific heat, we estimate the electron-phonon coupling constant λ to be of the order of 2, significantly enhanced compared to common weak-coupling values ≤ 0.4 . Our data also indicate that the electronic specific heat in the superconducting state of MgB₂ can be accounted for by a conventional, *s*-wave type BCS model.

DOI: 10.1103/PhysRevB.64.172515

PACS number(s): 74.25.Bt, 74.60.-w, 74.25.Kc

The recent discovery of superconductivity in MgB₂ below $T_c \approx 39$ K (Ref. 1) has caused a remarkable excitement in the solid-state physics community. Critical temperatures of this magnitude inevitably raise the question whether mechanisms other than the common electron-phonon interaction are responsible for the transition. In their very recent work, Bud'ko *et al.*² have investigated the Boron isotope effect in superconducting MgB₂ and found that replacing ¹¹B by ¹⁰B increases the critical temperature by about 1 K. This was taken as strong evidence that superconductivity in MgB₂ is of conventional nature, i.e., the electron pairing interaction is phonon mediated. Kotagawa *et al.* have interpreted their ¹¹B NMR measurements as indicating strong coupling *s*-wave superconductivity.³ Preliminary ¹¹B NMR measurements at low temperatures yield spectra which are consistent with the expectations for a type-II superconductor in the mixed state.⁴ Evidence for sizeable electron-phonon coupling is also provided by recent band-structure calculations.⁵⁻⁷ Various tunneling experiments have provided some evidence for conventional BCS-like superconductivity, but the values of the superconducting energy gap extracted from these measurements vary from 2 to 7 meV.⁸⁻¹⁰

In this paper, we report on measurements of the specific heat C_p of MgB₂ and present $C_p(T)$ data in a wide temperature range. Using a consistent model for the contribution of the lattice vibrations to $C_p(T)$ we calculate the electronic specific heat of this material. We show that the electronic specific heat below T_c is in good agreement with a conventional BCS-type interpretation.

The sample has been prepared from commercially available MgB₂ powder (Alfa Aesar) by sintering a pressed pellet at 500 °C for about 72 h. Electron microprobe investigations of the sample have shown that impurities of heavy elements (Cu, Ni, W) with concentrations of the order of 10^{-2} are present in the sample.

The specific heat $C_p(T)$ of the sintered MgB₂ sample has been measured using two different experimental techniques in overlapping temperature ranges. A standard relaxation technique was employed in the temperature range between 3 and 45 K. For temperatures between 20 and 220 K an adiabatic continuous heating calorimeter was used. Special care was taken to minimize the radiation losses at elevated

temperatures.¹¹ The temperatures in the range between 3 and 45 K were reached using a pumped ⁴He cryostat, and for those between 20 and 220 K, a conventional gas-flow ⁴He cryostat was used.

In the lower inset of Fig. 1 we show the magnetization of our sample divided by the constant applied field, M/H , as a function of temperature for $T < 50$ K. The superconducting transition temperature is 37.5 K and is indicated by the vertical arrow in the figure. The reduction of T_c of our sample, compared to $T_c \approx 39$ K observed by Bud'ko and co-workers,² is most likely due to the fact that our sample is not as clean as theirs and the superconducting transition temperature is slightly reduced by the impurities. We note, however, that the anomaly in $C_p(T)$ at T_c is at least as sharp as the one reported in Ref. 2.

In Fig. 1 we show the as measured specific heat $C_p(T)$ vs T in the whole temperature range covered in this study. The upper inset of this figure shows the same data in a limited temperature range around T_c . The anomaly in the specific heat due to the superconducting transition of MgB₂ at about 37.5 K is clearly resolved. We note that the absolute values of the data presented here are in good agreement with previously reported results of the specific heat of MgB₂ in a narrow range of temperatures around T_c .²

With respect to superconductivity in MgB₂, the most interesting part of $C_p(T)$ is the electronic specific heat $C_{el}(T)$. In order to reliably separate this contribution from the total, measured specific heat, the contribution due to lattice excitations, $C_{ph}(T)$, has to be known quite accurately. As may be seen in Fig. 1, the lattice provides the dominant contribution to the total, measured specific heat above 20 K. Well below the Debye-temperature θ_D , the specific heat in the normal state of a common metal is usually approximated by $C_p(T) = \gamma T + \beta T^3$, where the first term represents the electronic and the second term the lattice specific heat. We show below that this approximation for evaluating both, the electronic and the lattice specific heat, is not applicable for MgB₂ at $T \geq T_c$. Even at temperatures only slightly above T_c , the lattice specific heat may not simply be described by assuming a linear dispersion of the acoustic modes.

In Fig. 2, we show the total measured specific heat of MgB₂ divided by T^3 as a function of T . We note that, just

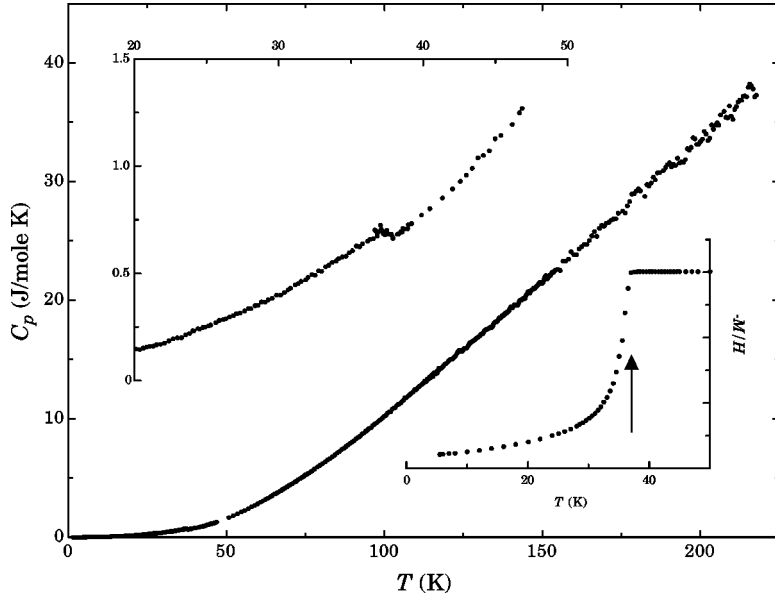


FIG. 1. Specific heat $C_p(T)$ of sintered MgB_2 as a function of temperature between 3 and 220 K. The absolute errors of the presented data are below 3% in the whole covered temperature range. The upper inset shows the same quantity in a limited temperature range. The lower inset displays the magnetization M divided by the applied field H as a function of temperature for our sample. The vertical arrow marks the onset of superconductivity in this material at $T_c \approx 37.5$ K.

above T_c , $C_p(T)/T^3$ increases with increasing temperature and passes through a pronounced local maximum at about 60 K. Such a feature cannot be described by the approximation $C_p(T) = \gamma T + \beta T^3$, mentioned above.

Due to the present lack of thermal expansion data, we cannot calculate the specific heat $C_V(T)$ at constant volume. The difference between $C_p(T)$ and $C_V(T)$ is expected to be small in the entire covered temperature range and at this point we neglect it.

We assume that the total specific heat at $T > T_c$ may be described by an electronic contribution $C_{el}(T)$ which is given by γT at $T > T_c$ in the whole covered temperature range, and a lattice contribution $C_{ph}(T)$.

The lattice specific heat is generally given by

$$C_{ph}(T) = \int_0^\infty d\omega g(\omega) \frac{\hbar^2 \omega^2}{k_B T^2} \frac{\exp\left(\frac{\hbar \omega}{k_B T}\right)}{\left(\exp\left(\frac{\hbar \omega}{k_B T}\right) - 1\right)^2}, \quad (1)$$

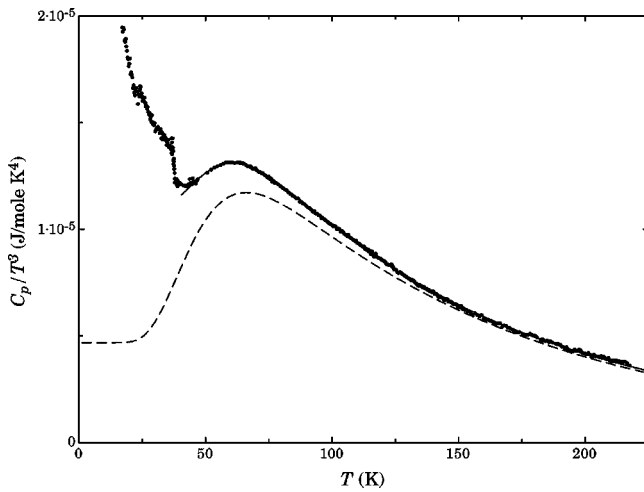


FIG. 2. Specific heat $C_p(T)$ of MgB_2 plotted as $C_p(T)/T^3$. The solid line represents a fit of Eq. (4) to the data at $T > T_c$, and the broken line represents the resulting lattice contribution (see text).

where $g(\omega)$ denotes the phonon density of states (PDOS), \hbar the Planck and k_B the Boltzmann constant, respectively. In the Debye approximation, the lattice is treated as an isotropic continuum with a linear dispersion, which leads to a PDOS proportional to ω^2 for $\omega < \omega_D$, ω_D denoting the cutoff frequency above which the PDOS is zero, and accordingly, to a low-temperature lattice specific heat of the form $C_{ph}(T)/T^3 = \text{const}$. As mentioned above, it is not possible to describe the observed maximum in $C_p(T)/T^3$ by this simple model. The Debye model may easily be extended to include deviations from the linear dispersion. This leads to a PDOS of the form $g(\omega) = \mu \omega^2 + \nu \omega^4$ and, in the low temperature limit, to $C_{ph}/T^3 = \beta + \delta T^2$. The cutoff frequency ω_D is chosen such that the total PDOS per mole is limited to $3pN_A$, where p is the number of atoms per unit cell and N_A Avogadro's constant. The lattice specific heat in this extended Debye scheme is then given by

$$C_D(T) = \int_0^{\omega_D} d\omega (\mu \omega^2 + \nu \omega^4) \frac{\hbar^2 \omega^2}{k_B T^2} \frac{\exp\left(\frac{\hbar \omega}{k_B T}\right)}{\left(\exp\left(\frac{\hbar \omega}{k_B T}\right) - 1\right)^2}. \quad (2)$$

Kortus and co-workers⁵ have recently computed the energies of the zone-center optical modes in MgB_2 using a frozen phonon scheme. According to their work, the lowest optical mode is doubly degenerate and located around an energy of $\hbar \omega_{opt}/k_B \approx 460$ K. A calculation of the phonon spectrum yields a peak in the PDOS at $\hbar \bar{\omega}_{opt}/k_B \approx 380$ K.⁶ Modes of this energy contribute to the lattice specific heat already at temperatures far below T_c and thus cannot be neglected in our analysis. In order to take them into account, we include their contribution into our approximation of the lattice specific heat by treating them as Einstein modes. The specific heat of one Einstein mode (N_A states at an energy $\hbar \omega_E$) is given by

$$C_{\text{opt}}(T) = N_A \frac{\hbar^2 \omega_E^2}{k_B T^2} \frac{\exp(\Theta_E/T)}{(\exp(\Theta_E/T) - 1)^2}, \quad (3)$$

where $\Theta_E = \hbar \omega_E / k_B$ denotes the Einstein temperature, and $\hbar \omega_E$ the energy of the optical mode.

MgB₂ has $p=3$ atoms per unit cell, and therefore 9 phonon modes. We treat the energetically lowest optical modes according to Eq. (3) and the remaining modes by the formula given in Eq. (2). The solid line in Fig. 2 is a fit based on

$$C_p(T)/T^3 = \gamma/T^2 + C_D(T)/T^3 + C_{\text{opt}}(T)/T^3 \quad (4)$$

to the data at $T > T_c$. By inspecting Fig. 2, it may be seen that with this model the measured total specific heat $C_p(T)$ may be well approximated at $T > T_c$, thus providing a rather accurate description of the lattice and the electronic specific heat of MgB₂ in its normal state. We note that the quoted fit parameters do not depend on the starting conditions of the fit.

The fitting procedure provides a value of 5.5 ± 0.2 mJ mol K² for γ . This value is almost twice as large as the γ value given in Ref. 2. However, considering the high accuracy of our fit we are confident that our value for γ is quite reliable. If we interpret the γ parameter as the Sommerfeld constant, a comparison with recently calculated densities of states at the Fermi energy E_F , $D(E_F) = 0.72$ states unit cell eV⁵ and 0.74 states unit cell eV,¹² respectively, leads directly to a value $m^*/m = 3.14$ for the average mass enhancement of the conduction electrons in MgB₂. Neglecting other many-body effects, the corresponding electron-phonon coupling constant $\lambda = m^*/m - 1 = 2.14$ is significantly enhanced above the usual BCS-weak-coupling values of $\lambda_{wc} < 0.4$, thus providing evidence for a considerable electron-phonon coupling in MgB₂.

The lattice contribution to the specific heat extracted from the fit is shown in Fig. 2 as a broken line. Since our model reproduces the total specific heat at elevated temperatures rather well, we may safely assume that our calculation provides the lattice contribution not only for $T > T_c$, but across the whole covered temperature range. The other two main parameters which emerge from the fit are the Debye temperature $\theta_D = 750 \pm 10$ K,¹³ in good agreement with the value given in Ref. 2, and the Einstein temperature $\theta_E = 325 \pm 5$ K. The corresponding energy for this dispersionless mode is in reasonable agreement with the position of the peak in the PDOS calculated in Ref. 6 and observed at $\hbar \omega / k_B = 365$ K in the inelastic neutron scattering data of Ref. 14.

With the proviso that the lattice specific heat $C_{\text{ph}}(T)$ is now established at all covered temperatures, we calculated the electronic specific heat of MgB₂ by subtracting $C_{\text{ph}}(T)$ from the total measured specific heat. The result of this calculation is shown in Fig. 3 by the closed circles.

As mentioned in the introduction it seems quite likely that superconductivity in MgB₂ is driven by conventional electron-phonon coupling. It has been shown that the specific heat of conventional, electron-phonon coupling driven superconductors is, regardless of the coupling strength, well described by the usual BCS expression, but scaled by the factor

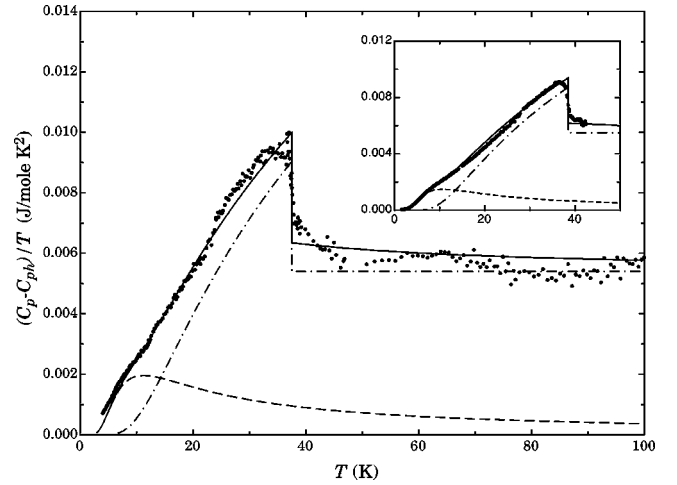


FIG. 3. Total specific heat $C_p(T)$ minus the lattice contribution $C_{\text{ph}}(T)$ divided by T vs temperature. The solid line represents a fit to our data using Eq. (6). The broken line represents the resonance contribution due to the impurities and the dash-dotted line the calculated electronic specific heat (see text). The inset shows the same quantities as the main figure but for a cleaner sample. Electron microprobe investigations revealed an impurity concentration of less than 0.5%, and the fit to the data using Eq. (6) yielded an impurity concentration of 0.33%.

$\alpha_s = \Delta(0)/1.76k_B T_c$.¹⁵ Therefore, the electronic specific heat at $T < T_c$ may be written as^{15,16}

$$C_s(T) = \left(\frac{\Delta(0)}{1.76k_B T_c} \right) \left(- \frac{D(E_F)(1+\lambda)}{T} \right) \times \int_{-\infty}^{\infty} d\epsilon \left(\epsilon^2 + \tilde{\Delta}^2 + \frac{1}{2k_B T} \frac{\partial \tilde{\Delta}^2}{\partial (k_B T)^{-1}} \right) \frac{\partial f}{\partial E}, \quad (5)$$

where $\Delta(0)$ denotes the superconducting energy gap at $T = 0$ K and $\tilde{\Delta}$ is the temperature dependent BCS gap function. This function has been tabulated by Mühlischlegel.¹⁷ The numerical evaluation of Eq. (5) is presented as the dash-dotted line in Fig. 3. We note that our data are not well reproduced in this way, but, as we show below, the apparent extra contribution is due to lattice excitations of the impurities.

As already mentioned above, our sample contains impurities at concentrations of the order of 1%. Since boron and also magnesium are rather light atoms, the identified impurity atoms are certainly much heavier. Heavy impurity atoms may cause resonances in the continuum of the phonon excitation spectrum at energies well below the energy of the lowest optical mode.¹⁸ In order to separate such contributions to the specific heat from the electronic specific heat, we fitted our data with an expression of the form

$$C_p(T) - C_{\text{ph}}(T) = C_{\text{el}}(T) + C_{\text{res}}(T), \quad (6)$$

where $C_{\text{el}}(T)$ for $T < T_c$ is given by Eq. (5) and for $T > T_c$ by γT . To keep the model as simple as possible, the contribution to the specific heat due to the resonant modes, $C_{\text{res}}(T)$, is taken into account by an Einstein term similar to Eq. (3).

The impurity concentration n_{imp} enters as an additional free parameter. The fit gives $n_{\text{imp}}=0.5\%$, in line with our expectations, a resonance energy of 30 K, and $\Delta(0)=1.2k_B T_c$. The ratio $\Delta(0)/k_B T_c$ is surprisingly small but, as has been shown by Swihart,¹⁹ even for substantially enhanced electron-phonon couplings, $\Delta(0)/k_B T_c$ may be reduced to below the original weak-coupling value of 1.76. This is particularly the case if low-energy dispersionless phonon modes are present. We note that a similar analysis of the low temperature specific heat of a cleaner sample with approximately half of the impurity concentration has led to the same conclusions (see inset of Fig. 3).

The presence of impurities does not significantly alter the total specific heat at elevated temperatures. Their contribution to the lattice specific heat above T_c is less than 10^{-3} and can safely be neglected in the calculation described above in fitting the specific heat at $T>T_c$.

In Fig. 4 we show the electronic contribution to the specific heat in the temperature range between 3 and 75 K, which is extracted from the total specific heat by subtracting the lattice contribution, including the small resonant term discussed above. The solid line in this figure is calculated using Eq. (5). We note a rather good agreement between the calculations and our data, which provides further evidence that superconductivity in MgB_2 is well described by the BCS approximation.

In conclusion, we have presented a detailed analysis of experimental specific heat data for MgB_2 , covering an extended range of temperatures. The lattice specific heat is compatible with a Debye temperature $\theta_D=750$ K. The electronic specific heat is rather well described by the BCS approximation, assuming a zero-temperature energy gap of $\Delta(0)=1.2k_B T_c$. Finally, we have obtained an electron-phonon coupling constant $\lambda\approx 2$, which is distinctly larger than the usual weak-coupling values. This value of λ should be considered as an upper limit. If the difference $C_p - C_v$, approximately linear in T , cannot be neglected, this would

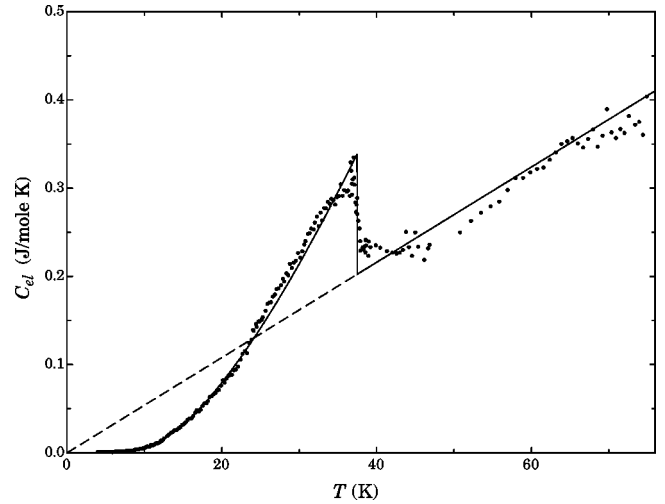


FIG. 4. Electronic specific heat $C_{\text{el}}(T)$ of MgB_2 as a function of temperature. The solid line represents the rescaled BCS expectation of the electronic specific heat [Eq. (5)], and the broken line is the electronic specific heat in the hypothetical normal state.

automatically lead to a reduction of λ . Indeed, with the published value for the bulk modulus $B=151$ GPa,²⁰ and a reasonable value for the volume thermal expansion coefficient $b=2.5\times 10^{-5}$ K^{-1} at $T>T_c$, we obtain $(C_p - C_v)/T = 1.67$ mJ mol K^2 . This would lead to a reduction of the electronic specific heat coefficient to $\gamma=3.83$ mJ/mol K^2 and a corresponding reduction of λ to a value of 1.18. According to Eq. (5), the ratio $\Delta(0)/k_B T_c$ would thus be enhanced to a value of 1.73.

The samples used in this work were prepared by S. Sigrist. We acknowledge the microprobe analysis investigations by P. Wägli. This work was in part financially supported by the Schweizerische Nationalfonds zur Förderung der wissenschaftlichen Forschung.

- ¹J. Akimitsu, Symposium on Transition Metal Oxides, Sendai (2001).
- ²S.L. Bud'ko, G. Lapertot, C. Petrovic, C.E. Cunningham, N. Anderson, and P.C. Canfield, Phys. Rev. Lett. **86**, 1877 (2001).
- ³H. Kotegawa, K. Ishida, Y. Kitaoka, T. Muranaka, and J. Akimitsu, cond-mat/0102334, Phys. Rev. Lett. (to be published).
- ⁴J.L. Gavilano, D. Rau, Sh. Mushkolaj, and H.R. Ott (private communication).
- ⁵J. Kortus, I.I. Mazin, K.D. Belashchenko, V.P. Antropov, and L.L. Boyer, Phys. Rev. Lett. **86**, 4656 (2001).
- ⁶Y. Kong, O.V. Dolgov, O. Jepsen, and O.K. Andersen, Phys. Rev. B **64**, 020501 (2001).
- ⁷J.M. An and W.E. Pickett, Phys. Rev. Lett. **86**, 4366 (2001).
- ⁸G. Rubio-Bollinger, H. Suderow, and S. Vieira, Phys. Rev. Lett. **86**, 5582 (2001).
- ⁹H. Schmidt, J.F. Zasadzinski, K.E. Gray, and D.G. Hinks, Phys. Rev. B **63**, 220504 (2001).

- ¹⁰A. Sharoni, I. Felner, and O. Millo, Phys. Rev. B **63**, 220508 (2001).
- ¹¹O. Jeandupeux, Ph.D. thesis, ETH Zürich, 1996.
- ¹²B. Delley and R. Monnier (unpublished).
- ¹³In our approach, Θ_D is a free fit parameter entering the parameter μ in Eq. (2).
- ¹⁴T.J. Sato, K. Shibata, and Y. Takano, cond-mat/0102468, (unpublished).
- ¹⁵H. Padamsee, J.E. Neighbor, and C.A. Shiffman, J. Low Temp. Phys. **12**, 387 (1973).
- ¹⁶G. Rickayzen, in *Superconductivity*, edited by R.D. Parks (Dekker, New York, 1969), p. 79.
- ¹⁷B. Mühlischlegel, Z. Phys. **155**, 313 (1959).
- ¹⁸C.T. Walker and R.O. Pohl, Phys. Rev. **131**, 1433 (1963).
- ¹⁹J.C. Swihart, Phys. Rev. **131**, 73 (1963).
- ²⁰T. Vogt, G. Schneider, J.A. Hriljac, G. Yang, and J.S. Abell, Phys. Rev. B **63**, 220505 (2001).